Technical Report

Department of Computer Science
and Engineering
University of Minnesota
4-192 Keller Hall
200 Union Street SE
Minneapolis, MN 55455-0159 USA

TR 15-014

Gathering Bearing Data for Target Localization

Haluk Bayram, Joshua Vander Hook, Volkan Isler

September 28, 2015

Gathering Bearing Data for Target Localization

Haluk Bayram, Joshua Vander Hook, Volkan Isler

***Abstract*— We consider the problem of gathering bearing data in order to localize targets. We start with a commonly used notion of uncertainty based on Geometric Dilution of Precision (GDOP) and study the following bi-criteria problem. Given a set of potential target locations and an uncertainty level U, compute an ordered set of measurement locations for a single robot which (i) minimizes the total cost given by the travel time plus the time spent in taking measurements, and (ii) ensures that the uncertainty in estimating the target's location is at most U regardless of the targets' locations. We present an approximation algorithm and prove that its cost is at most 28.9 times the optimal cost while guaranteeing that the uncertainty is at most $5.5U$. In addition to theoretical analysis, we validate the results in simulation and experiments performed with a directional antenna used for tracking invasive fish.**

I. Introduction

This paper considers the problem of controlling a mobile robot whose task is to cover an environment so as to estimate locations of one or more targets dispersed across the environment. We focus on a novel version of this general coverage problem in which the robot can collect only bearing measurements. Therefore, it must collect multiple measurements and estimate the targets' positions. The problem we study is to compute a coverage path as well as sensing locations along the path as shown in Figure 1. The goal is to guarantee that the uncertainty in each position estimate does not exceed a given bound while minimizing the data collection time.

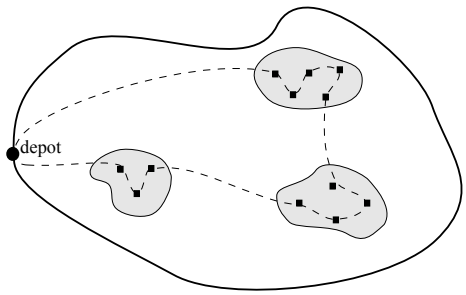

Fig. 1. Gathering Bearing Data: Shaded areas are the input regions which need to be searched. The goal is to compute measurement locations (squares) and a tour (dashed line) along them so that no matter where the targets are, the uncertainty in localizing them is small.

Robot coverage is a fundamental robotics problem which has been studied extensively [1]. In the traditional coverage problem, in order to cover a point, it suffices to "sense" it by visiting a point within the sensing range. However, if the robot can take only bearing measurements, at least two measurements must be taken. The uncertainty in localizing a target at location x is a function of not only distance but also the angle $\measuredangle s_1 x s_2$ where s_1 and s_2 are the two measurement locations [2].

The authors are with the Department of Computer Science & Engineering, University of Minnesota, Minneapolis, USA. This work was supported by National Science Foundation Awards #1111638, #0917676, and #1317788. {bayram, jvander, isler}@cs.umn.edu

Fig. 2. Robotic systems for finding and tracking radio-tagged invasive fish.

There are very few coverage results under the bearing-only sensing model. In [3], a greedy algorithm is developed to localize a target with a single mobile bearing-only sensor. A lower bound on the optimal localization time was derived, and used to bound the performance of the algorithm with respect to this bound. In [4], a similar algorithm was used to locate a dense cluster of targets. The targets were assumed to be close to each other and no guarantee of the time required to locate the targets was provided. Borri et. al [5] consider a mobile robot collecting measurements from a *fixed set* of possible locations in a bounded environment. We relax these restrictions to optimize the tour directly and consider localization of multiple targets.

The work in [6] studied the problem of placing stationary bearing sensors. Specifically, the authors studied the problem of placing a minimum number of sensors to guarantee that the uncertainty everywhere in the workspace is below a given threshold $U^\star$. They presented an algorithm which places $3k$ sensors and achieves $5.5U^\star$ uncertainty everywhere in the workspace where k is the optimal solution.

This work is motivated by our efforts to track radio-tagged carp in Minnesota lakes [7]. We use robotic boats in the summer and ground vehicles in the winter when the lakes are frozen (Figure 2). Both vehicles are equipped with directional antennas which are rotated to obtain bearing measurements. The fish loiter for extended periods of time, and their motion is relatively small compared to the sensing range. This is especially true in the winter when they aggregate [8]. Therefore they can be treated as stationary targets. The algorithm presented in this paper would be applicable in other settings for example for localizing unknown signal

sources [9], [10], [11].

In this paper, we study the problem for the case of a single, mobile bearing-only sensor trying to locate targets dispersed across an arbitrary but bounded subset of the plane. We proceed as follows. In Section II, we provide the basics of bearing-based target localization and present the uncertainty measure used throughout the paper. In Section III, we present the data gathering strategy and analyze its performance. In Section IV, the uncertainty measure and sensor placement algorithm are validated in simulation. Next, in Section V, we test the placement algorithm and sensor noise model in real-world field experiments.

II. Preliminaries

A. Uncertainty Model

Triangulation is commonly used in estimating the location of a target from two bearing measurements. The accuracy of the estimation depends on the target-sensor geometry and the environment. A common method to measure the uncertainty of the estimate is to use the geometric dilution of precision (GDOP). Consider two measurements from locations s_1 and s_2 for a target at location w. It is well known that the uncertainty is proportional to:

$$U(s_1, s_2, w) \propto \frac{d(s_1, w)d(s_2, w)}{|sin\measuredangle s_1 w s_2|} \tag{1}$$

where $d(s_i, w)$ denotes the distance between robot s_i and target location w. See e.g. [2].

The GDOP function can be extended to obtain the uncertainty in estimating the target's position for a given noise level in the bearing measurements by using the Fisher Information Matrix (FIM) [12]. Let I_θ denote the FIM for a given target-measurement geometry. The square roots of the eigenvalues of I_θ^{-1} denote the lengths of the axes of the target covariance. The determinant of the FIM can be regarded as a computable measure of the area of the ellipse. Given two bearing measurements for a target w, the determinant of the FIM is given as [12]:

$$det(I_\theta) = \frac{1}{\sigma^4} \frac{sin^2\measuredangle s_1 w s_2}{d(s_1, w)^2 d(s_2, w)^2} \tag{2}$$

where σ is the standard deviation of the noise in the bearing measurements. Since the determinant is the product of the eigenvalues, taking the reciprocal of both sides, followed by taking their square root yields:

$$\begin{aligned} \lambda_1\lambda_2 &= \frac{1}{\sigma^4} \frac{sin^2\measuredangle s_1 w s_2}{d(s_1, w)^2 d(s_2, w)^2} \\ \frac{1}{\lambda_1\lambda_2} &= \frac{d(s_1, w)^2 d(s_2, w)^2}{sin^2\measuredangle s_1 w s_2} \sigma^4 \\ \frac{1}{\sqrt{\lambda_1\lambda_2}} &= \frac{d(s_1, w)d(s_2, w)}{|sin\measuredangle s_1 w s_2|} \sigma^2 \end{aligned} \tag{3}$$

If we multiply both sides by π, the left hand side will give the area of the uncertainty ellipse, whose axes are of length $1/\sqrt{\lambda_1}$ and $1/\sqrt{\lambda_2}$. Hence, for a given noise level σ, the uncertainty becomes

$$U_\sigma(s_1, s_2, w) = \frac{d(s_1, w)d(s_2, w)}{|sin\measuredangle s_1 w s_2|} \pi\sigma^2 \tag{4}$$

B. Problem Statement

Let $\mathcal{T} \subseteq \mathbb{R}^2$ be a given set of candidate target locations. $\mathcal{T}$ can be an arbitrary, potentially disconnected, subset. In the fish tracking application, $\mathcal{T}$ can be the entire lake or a collection of regions where the fish are likely to be. A single robot equipped with a bearing sensor is charged with taking sensor measurements. The noise in bearing measurements is assumed to be mutually independent and normally distributed with zero mean and σ^2 variance. Each measurement takes τ time units which can be zero.

A *data gathering tour* S is a set of ordered measurement locations $S = \{s_1, s_2, \ldots s_n\}$. The cost of S is given by

$$cost(S) = \sum_{i=0}^{n-1} d(s_i, s_{i+1}) + n\tau \tag{5}$$

The first term in Eq. 5 corresponds to time spent in traveling whereas the second term corresponds to the total measurement time. To simplify the notation, we define $s_0 = s_n$. For any given point x, we define $U_\sigma(S, w)$ as $\min_{s,s' \in S} U_\sigma(s, s', w)$ – i.e. the uncertainty achieved by the best pair in S.

In this paper, we study the following problem:

Problem 1: Given an environment $\mathcal{T}$, initial position s_0 and measurement error variance σ^2, compute a data gathering tour S such that $cost(S)$ is minimized, *and* for each location $w \in \mathcal{T}$, there exist $s_i, s_j \in S$ such that $U_\sigma(s_i, s_j, w)$ is less than a given threshold $U^\star$.

Our main result is an algorithm which computes a tour whose cost is at most 28.9 times the optimal cost while guaranteeing that the localization uncertainty is at most $5.5U^\star$. In obtaining this result, we use the following results from previous work which will be used in the analysis.

The sensor placement scheme in [6] proceeds as follows: Given the environment $\mathcal{T} \subseteq \mathbb{R}^2$, an uncertainty threshold $U^\star$, and a bearing noise variance σ^2, Algorithm 1 determines the locations of the sensors. Throughout the paper, let $D(x, a)$ be a disk centered at x with radius a.

The authors then show the following result:

Lemma 1 ([6]): For any $x \in \mathcal{T}$ and any $y \in D(x, 2R)$, $U(S(x), y)$ is less than $5.5U^\star$.

The second result we will use is related to a variant of the well-known Traveling Salesperson Problem (TSP) known as TSP with Neighborhoods (TSPN). In a geometric version of TSPN, we are given n uniform disks. The goal is to compute the shortest tour which visits at least one point in each disk.

Lemma 2 ([13]): Let $\mathcal{D}$ be a set of n disjoint disks with radius R. Any tour τ of $\mathcal{D}$ satisfies $|\tau| \geq \frac{n}{2}\alpha R$ where $\alpha = 0.4786$ and $n \geq 3$.

Algorithm 1 *PlaceSensors*

Input: $\mathcal{T}$, $U^\star$ and σ^2

$R \leftarrow \sqrt{U^\star/(\pi\sigma^2)}$
$R' \leftarrow 2R/\sqrt[3]{4}$
$\mathcal{S} \leftarrow \emptyset$
$\mathcal{D} \leftarrow \emptyset$
while $\mathcal{T} \neq \emptyset$ **do**
  Pick an arbitrary point x in $\mathcal{T}$
  $D(x, R) \leftarrow$ a disk with radius R around x
  $C(x, R') \leftarrow$ a circle centered at x with radius R'
  $s_i \leftarrow$ a point on C at angle $(i-1)2\pi/3$, $i = 1, 2, 3$
  $S(x) \leftarrow \{s_1, s_2, s_3\}$
  $\mathcal{D} \leftarrow \mathcal{D} \cup D(x, R)$
  $\mathcal{S} \leftarrow S \cup S(x)$
  $\mathcal{T} \leftarrow \mathcal{T} \setminus D(x, 2R)$
end while

Output: $\mathcal{S}$ and $\mathcal{D}$

III. Gathering Bearing Data

Our algorithm *GatherData* proceeds as follows: Given the environment $\mathcal{T}$ and the uncertainty threshold $U^\star$, we first run the Algorithm *PlaceSensors* (Algorithm 1) to obtain sensor locations given by $S = \cup S(x)$ where $x \in \mathcal{T}$. *GatherData* computes a TSP tour of these points and outputs them in the order given by the tour.

In general, picking sensing locations independent of the tour can yield arbitrarily bad results. We show that by picking the sensor locations carefully, we can bound the deviation from the optimal tour.

Let OPT be the optimal solution for gathering data under the cost function given in Equation 5. We show that the cost of the resulting tour is within a constant factor of the cost of OPT. For analysis purposes, we split the cost term into travel time and measurement time and use the subscripts d for travel (distance) and m for measurement time. That is, OPT_d denotes the cost incurred by OPT for traveling, and OPT_m is the time spent in taking measurements.

The key observation is the following:

Proposition 1: Let $\mathcal{D}$ be the set of disks generated by *PlaceSensors*. OPT must take at least one measurement from each disk in $\mathcal{D}$.

Proof: Suppose the statement is false and that there is an optimal solution in which all measurements are taken outside of a particular disk generated by *PlaceSensors*. Let w be the center of this disk. Note that $w \in \mathcal{T}$. Let s_1 and s_2 be the two locations in OPT associated with w. We have

$$\begin{aligned}\frac{d(s_1,w)d(s_2,w)}{|sin\angle s_1 w s_2|}\pi\sigma^2 &> \frac{\sqrt{U^\star/(\pi\sigma^2)}\sqrt{U^\star/(\pi\sigma^2)}}{|sin\angle s_1 w s_2|}\pi\sigma^2 \\ &\geq \sqrt{U^\star/(\pi\sigma^2)}\sqrt{U^\star/(\pi\sigma^2)}\pi\sigma^2 \\ &= U^\star\end{aligned}$$

which contradicts the fact that OPT satisfies the desired level of uncertainty for location w. ■

Proposition 1 yields the following corollary.

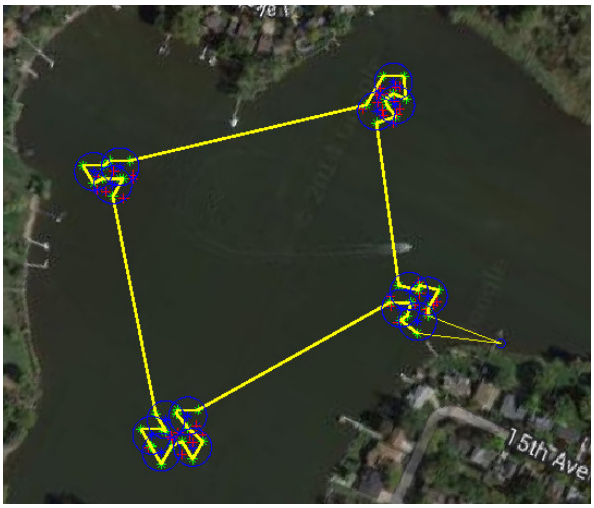

Fig. 3. A simulated example tour generated by the algorithm. The four areas are known to contain targets, and a sensing tour is computed to localize all the targets. Theorem 1 shows that the tour of the measurement locations is near optimal, and Lemma 1 shows that any target in the area will be localized to desired uncertainty. The green crosses are computed measurement locations, the yellow path is the tour, and the red crosses are the target locations.

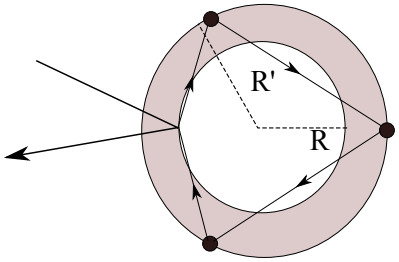

Fig. 4. A TSPN tour can be converted to a TSP tour visiting the sensing locations as shown in the figure. Every time we visit a disk, we take a detour and visit the three sensor locations associated with it.

Corollary 1: Let $\mathcal{D}$ be the set of disks generated by *PlaceSensors*. OPT is a TSPN tour for $\mathcal{D}$.

Theorem 1: Let SOL be the cost of the tour generated by *GatherData*. $SOL \leq (1 + \frac{2\beta}{\alpha})OPT = 28.9OPT$ where $\beta = 6.6687$, $\alpha = 0.4786$ and OPT is the optimal data gathering tour.

Proof: Let $TSPN$ be the optimal TSPN tour visiting disks in $\mathcal{D}$. Since OPT also visits these disks (Proposition 1) we have

$$OPT_d \geq TSPN \quad (6)$$
$$\geq \frac{n}{2}\alpha R \quad (7)$$

where n is the number of disjoint disks with radius R and the second inequality follows from Lemma 2.

Let SOL_d denote the cost of the optimal TSP tour generated by our algorithm in terms of distance. Now, we have

$$SOL_d \leq TSPN + n\beta R \quad (8)$$

Here βR is the cost of going from the boundary of a disk to the first sensor location and then to the second, third and

coming back. Fig. 4 depicts the maximum distance for this process. This occurs when the TSPN visits a point equidistant from two sensor locations. Hence, the total distance βR will be

$$\beta R = 2\sqrt{3}R' + 2\sqrt{3R'^2/4 + (R - R'/2)^2} \quad (9)$$

where $R' = 2R/\sqrt[3]{4}$. After substituting R' into Eq. 9, we get $\beta = 6.668$.

The reason why the inequality in Eq. 8 holds is that starting from any TSPN solution for $\mathcal{D}$, we can obtain a TSP tour of the sensing locations in SOL as follows: when a disk is visited, visit the the three sensor locations associated with this disk. Since SOL_d is the cost of the optimal TSP tour of these locations, it is a lower bound on the cost of any TSP tour.

Now, substituting Eq. 6 and Eq. 7 into Eq. 8, we obtain

$$\begin{aligned} SOL_d &\leq TSPN + n\beta R \\ &\leq OPT_d + \frac{2\beta}{\alpha} OPT_d \\ &\leq (1 + \frac{2\beta}{\alpha}) OPT_d \end{aligned}$$

Hence $1 + \frac{2\beta}{\alpha}$ is the approximation ratio when only considering the distance factor in the cost function.

We now bound the measurement time. Since the disks are disjoint and OPT must take at least one measurement in each disk as stated in Proposition 1, its measurement time is at least $n\tau$. Since the measurement time for our algorithm is $3n\tau$, we obtain:

$$SOL_m \leq 3OPT_m \quad (10)$$

Therefore we have the total cost as

$$\begin{aligned} SOL &= SOL_d + SOL_m \leq (1 + \frac{2\beta}{\alpha}) OPT_d + 3OPT_m \\ &\leq (1 + \frac{2\beta}{\alpha}) OPT \end{aligned}$$

and the result follows. ■

IV. Simulations

In this section we validate the sensor model and the subroutine *PlaceSensors* in simulations. For this purpose, we evaluate simulated instances for varying bearing noise $\sigma = \{\pi/36, \pi/18, \pi/12, \pi/9\}$ radians and uncertainty thresholds $U^\star = \{4, 8, 16, 32, 64, 128\}$. In each simulation, a target location is chosen uniformly at random within the measurement area defined by a circle with radius $2R = 2\sqrt{U^\star/(\pi\sigma^2)}$. The sensors are placed according to *PlaceSensors*. Each sensor obtains a single noisy measurement. An iterative batch estimator is used to find the maximum likelihood estimate of the target's location. The estimation process is described in [14] (See Chapter 3 for an accessible introduction).

This process is repeated 1000 times. For each scenario, we compute the mean area and estimation error. The uncertainty area is calculated as $\pi\sqrt{det(\Sigma)}$, for covariance Σ, which is the area of the uncertainty ellipse.

A sample scenario with $U^\star = 32$ and $\sigma = \pi/12$ is shown in Fig. 5(a). Each sensor location is shown as a blue solid circle. A black square denotes true target position and a red cross is the estimate. The uncertainty area is shown by a red ellipse. For this scenario, Fig. 5(b) shows the uncertainty ellipses for 1000 random target locations with $U^\star = 32$ and $\sigma = \pi/12$. Only 4 samples out of 1000 exceed the threshold value of $5.5U^\star = 177$. In those four samples, high measurement noise had placed the target estimate outside of the circle. Thus, the estimated uncertainty for the target hypothesis was large.

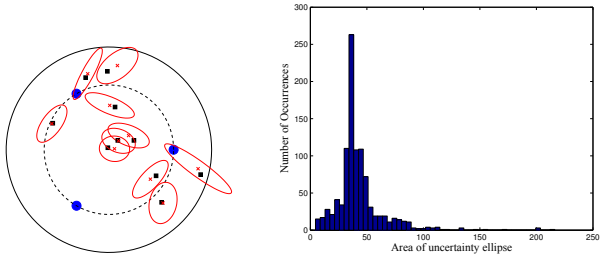

(a) (b)

Fig. 5. (a) A sample scenario with $U^\star = 32$ and $\sigma = \pi/12$. Each measurement location is shown by blue solid circle. Black squares denote true target positions. Red crosses are the positions of the estimates. Uncertainty areas is shown as red ellipses. (b) Number of occurrences of areas of the uncertainty ellipses for 1000 random target locations with $U^\star = 32$ and $\sigma = \pi/12$.

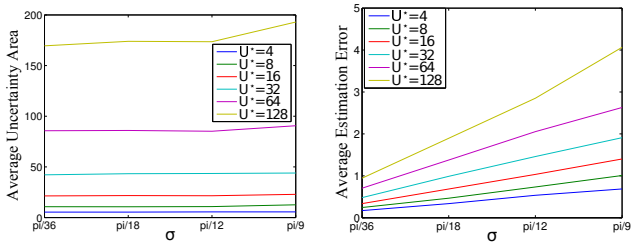

(a) (b)

Fig. 6. (a) Average uncertainty area and (b) average estimation error for varying the uncertainty threshold $U^\star$ and the measurement noise σ.

Statistical results are as shown in Fig. 6(a) and 6(b). It is observed that for a given uncertainty threshold $U^\star$, the resulting average uncertainty area becomes almost constant with increasing noise. The average uncertainty area is far below the threshold $5.5U^\star$, which verifies Lemma 1. According to Fig. 6(b), estimation error gets more noise-sensitive when the uncertainty threshold increases. For instance, while the slope of the average estimation error is approximately 2 when $U^\star = 4$, the slope is 4 for $U^\star = 128$.

V. Field Experiments

A. Sensing Model Validation

Our study is motivated by a real-world application: tracking radio-tagged invasive fish with a radio antenna system. As mentioned, the fish in question tend to aggregate in stationary groups. Thus, the goal of our field test is to verify

(a) A radio transmitter.

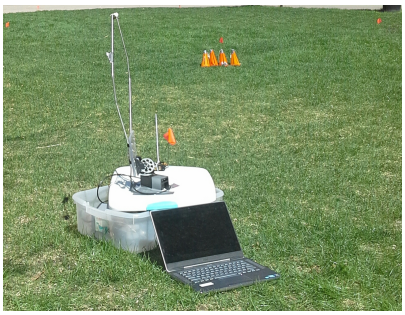

(b) The field experimental setup.

Fig. 7. (a) A tag sends an uncoded transmission on a specific frequency once per second. (b) The antenna is shown in the foreground, and radio transmitters were placed in the field nearby. A direction-sensitive antenna is rotated to estimate the bearing to the transmitting radio tag. The signal strength is strongest when the plane of the antenna loop is roughly aligned with the tag.

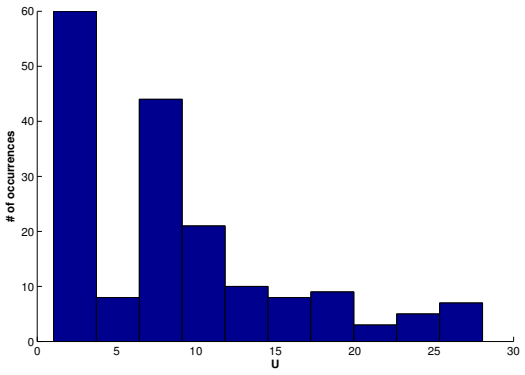

Fig. 8. Number of occurrences of areas of the uncertainty ellipses for the experiment results with $U^\star = 2.5$ and $\sigma = \pi/18$.

the radio tags shown in Figure 7(a) can be located using estimates of bearings constructed from three radio antennas. The sensor, a direction-sensitive radio antenna connected to a pan-tilt servo, was developed for the robotic system described in [7] and is shown detached from the system in Figure 7(b).

First, we did systematic experiments in a grassy field so as to evaluate the overall performance of the approach. For this purpose, we divide the environment equally into square cells with edges of 5-meter length as shown in Figure 9, hence we have 25 locations for radio tags. 7 tags with different frequencies are placed at each corner of the cells. We have assumed the measurement noise of $\sigma = \pi/18$ rad, which is consistent with the previous work in [3], and the uncertainty U is set to 2.5. Using Lemma 1, the radius of the circle on which three sensors are located is calculated as $R' = 6$ meters, the radius of the measurement area within which the uncertainty is less than $5.5U$ is equal to $2R = 10$ meters. Three measurements are taken for each radio tag from three sensor locations on a circle of radius $R' = 6$ meters.

The estimated target positions are plotted in Figure 9 along with the measured ground-truth locations. The sensor locations are shown as blue circles, target estimates are black x's. For each target position inside the circle with radius

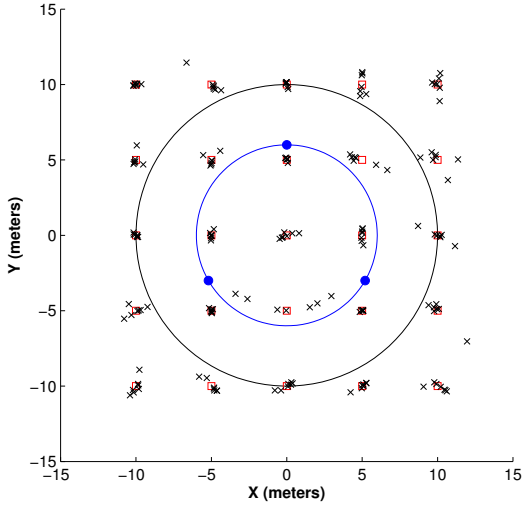

Fig. 9. Actual and estimated positions for the field experiment results. Each measurement location is shown by a blue solid circle. Red squares show true target positions and black crosses show estimate positions.

Fig. 10. Lake experiment: gathering bearing data on a windy day.

$R = 10$ meters, the uncertainty U is less than $5.5U^\star$.

B. Lake Experiments

We report results from a set of tests conducted on two different days at Lake Staring in MN, USA. The robot (OceanScience QBoat) shown in Figure 10 was used in the experiments. The boat was augmented with an on-board laptop and motor control board for autonomous navigation, and a pan-tilt servo, antenna, and real-time spectral analyzer to produce bearing measurements. It is 2 meters in length and has an average speed of 1 meter per second.

The tags were deployed at a known location within a measurement area. Due to the wind affecting the boat's navigation and cloud cover affecting GPS signals, the uncertainties on the localization will increase. Hence, the uncertainty threshold $U^\star$ was set to 4.5 in the first day experiment. Under these conditions, the radius of the measurement area is equal to 14 meters. Figure 11 shows one of the trials. In these experiments, the boat started navigating to its measurement locations (square symbols) from the location shown as the star. The cross symbol represents the estimated target position and the diamond symbol shows the true target location. The uncertainty U is about 19.3, which is less than $5.5U^\star$.

We have also conducted experiments with two measurement regions on the second day. This day was even windier

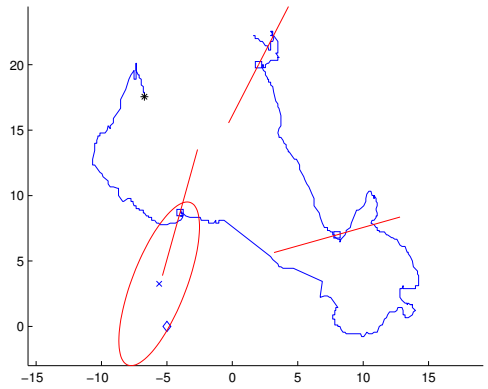

Fig. 11. Actual and estimated positions for a lake experiment result. The measurement locations are denoted by square. While the diamond denotes true target position, the cross estimate position.

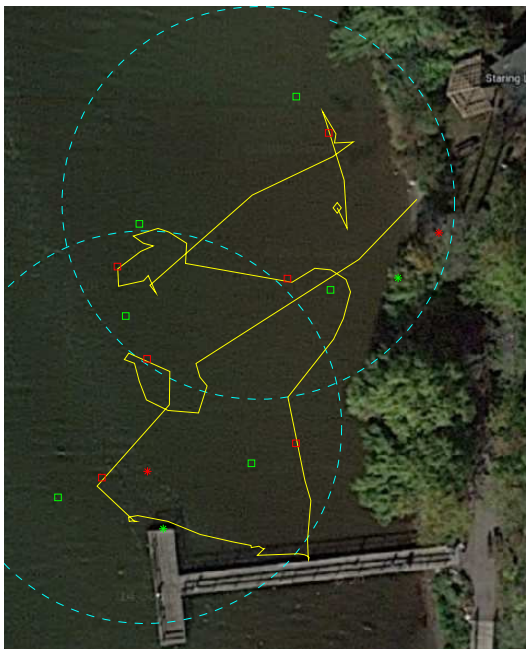

Fig. 12. Two measurement regions. Green and red squares denote the desired and actual measurement locations, respectively. While green stars denote true target positions, red stars estimate position. The boat began from the location labeled with the yellow diamond and followed the yellow trajectory. The boundary of the measurement regions is denoted by dashed line.

(Figure 10 shows a snapshot). Therefore, the measurement noise σ was changed from $\pi/18$ to $\pi/12$ and the uncertainty threshold $U^\star$ was set to 20. One of these experiments can be seen in Figure 12. The targets were localized with an error of approximately 6 meters.

In conclusion, the simulation results indicate that the proposed approach enables us to analyze the relationship between the bearing noise σ and uncertainty threshold $U^\star$. Given a fixed $U^\star$, the estimation performance is robust to the change in the bearing noise. The practical applicability of the proposed approach has been also tested in a series of experiments with an autonomous boat. The experiments have demonstrated the effectiveness of the proposed approach even under other uncertainties such as wind and GPS errors.

VI. Conclusion

This paper considered the problem of gathering bearing data with a mobile robot so as to estimate the positions of targets located in a given environment. We presented a constant factor approximation algorithm which guarantees that the cost of gathering data is within factor 28.9 of the optimal solution and the uncertainty is within a factor 5.5. These two factors can be traded off to guarantee, for example, the same level of uncertainty with the optimal solution at the expense of increased cost. We leave the analysis of this trade-off for future work.

In the field experiments, an autonomous boat was able to localize the transmitting radio tag within a desired uncertainty. Our future work also includes data gathering with multiple robots.

References

[1] E. Galceran and M. Carreras, "A survey on coverage path planning for robotics," *Robotics and Autonomous Systems*, vol. 61, no. 12, pp. 1258 – 1276, 2013.

[2] A. Kelly, "Precision dilution in triangulation based mobile robot position estimation," in *Proceedings of the International Conference on Intelligent Autonomous Systems*, Amsterdam, 2003.

[3] J. Vander Hook, P. Tokekar, and V. Isler, "Cautious greedy strategy for bearing-only active localization: Analysis and field experiments," *Journal of Field Robotics*, vol. 31, no. 2, pp. 296–318, 2014.

[4] J. Vander Hook, P. Tokekar, E. Branson, P. G. Bajer, P. W. Sorensen, and V. Isler, "Local-search strategy for active localization of multiple invasive fish," in *Experimental Robotics*, B. Siciliano and O. Khatib, Eds., vol. 88. Springer Tracs in Advanced Robotics, 2013, pp. 859–873.

[5] A. Borri, S. D. Bopardikar, J. P. Hespanha, and M. D. Di Benedetto, "Hide-and-Seek with Directional Sensing," in *Proceedings of the 18th IFAC World Congress, Milan, Italy*, 2011, pp. 9343–9348.

[6] O. Tekdas and V. Isler, "Sensor placement for triangulation-based localization," *Automation Science and Engineering, IEEE Transactions on*, vol. 7, no. 3, pp. 681–685, July 2010.

[7] P. Tokekar, E. Branson, J. Vander Hook, and V. Isler, "Tracking aquadic invaders: Autonomous robots for monitoring invasive fish," *IEEE Robotics and Automation Magazine*, vol. 20, no. 3, pp. 33–41, September 2013.

[8] P. G. Bajer, H. Lim, M. J. Travaline, B. D. Miller, and P. W. Sorensen, "Cognitive aspects of food searching behavior in free-ranging wild common carp," *Environmental Biology of Fishes*, vol. 88, no. 3, pp. 295–300, 2010.

[9] B. A. E. Frew, C. Dixon and T. Brown, "Radio source localization by a cooperating uav team," in *Infotech@Aerospace*, 2005, pp. 1–11.

[10] K. Mcgill and S. Taylor, "Robot algorithms for localization of multiple emission sources," *ACM Comput. Surv.*, vol. 43, no. 3, pp. 15:1–15:25, 2011.

[11] D. Song, C.-Y. Kim, and J. Yi, "Simultaneous localization of multiple unknown and transient radio sources using a mobile robot," *Robotics, IEEE Transactions on*, vol. 28, no. 3, pp. 668–680, June 2012.

[12] A. N. Bishop, B. Fidan, B. D. Anderson, K. Dogancay, and P. N. Pathirana, "Optimality analysis of sensor-target localization geometries," *Automatica*, vol. 46, no. 3, pp. 479–492, 2010.

[13] O. Tekdas, D. Bhadauria, and V. Isler, "Efficient data collection from wireless nodes under the two-ring communication model," *The International Journal of Robotics Research*, vol. 31, no. 6, pp. 774–784, 2012.

[14] Y. Bar-Shalom, X.-R. Li, and T. Kirubarajan, *Estimation with Applications to Tracking and Navigation*. New York, USA: John Wiley & Sons, Inc., 2001.